

JUL 15 1959 RECEIVED

NASA 00-E
438

MASS TRANSFER, FLOW, AND HEAT TRANSFER ABOUT A ROTATING DISK

For presentation
at 1959 ASME
Annual Meeting,By E. M. Sparrow and J. L. Gregg, Associate Members, ASME
NASA, Lewis Research Center, Cleveland, OhioAtlantic City, December and for ABSTRACT
publication in the Journal of Heat Transfer.

The effects of mass injection or removal at the surface of a rotating disk on

heat transfer and on the flow field about the disk are studied. Consideration is given to gaseous systems which are composed of either one or two component gases.

Solutions of the equations which govern the hydrodynamics, energy transfer, and mass diffusion have been obtained over the entire range from large suction velocities to large blowing velocities. Results are given for the velocity, temperature, and mass fraction distributions, as well as for the heat transfer, mass transfer, and torque requirements. The effects of the mass transfer are discussed in detail. It is shown that fluid injection sharply decreases the heat transfer at the surface.

NOMENCLATURE

c_p	specific heat at constant pressure
D	coefficient of diffusion
F, G, H	dimensionless velocity variables defined in equation (9b)
h	heat transfer coefficient, $q/(T_w - T_\infty)$
k	thermal conductivity
M	torque
m	rate of mass flow
Nu	Nusselt number, $h \left(\frac{v}{\omega} \right)^{1/2} / k$
P	dimensionless pressure defined by equation (9b)
Pr	Prandtl number, $\nu/\alpha = c_p \mu / k$
q	heat transfer rate per unit area
r	radial coordinate
Sc	Schmidt number, ν/D
T	static temperature
V_r, V_ϕ, V_z	convective velocity components

FACILITY FORM 502

N65 83014

(ACCESSION NUMBER)

30

(PAGES)

TMX #56177

(NASA CR OR TMX OR AD NUMBER)

(THRU)

Kong

(CODE)

(CATEGORY)

NASA FILE 000

loan expires on last

date stamped on back cover

PIL 10-10-10-10

DWM 10-10-10-10

30-10-10-10

30-10-10-10

Washington 25

NASA TMX # 56177

mclaguerney
ATSD

3/31/65

E-438

v_r, v_ϕ, v_z	diffusive velocity components
W_i	mass fraction, ρ_i/ρ
z	coordinate measuring distance normal to disk surface
α	thermal diffusivity
δ	thickness of viscous or thermal layers (see subscripts)
η	dimensionless independent coordinate, $(\omega/\nu)^{1/2} z$
θ	dimensionless temperature, $(T - T_\infty)/(T_w - T_\infty)$
μ	absolute viscosity
ν	kinematic viscosity
ρ	density
τ_ϕ, τ_r	shear stress components at the disk surface
Φ	dimensionless mass fraction, $(W_1 - W_{1\infty})/(W_{1w} - W_{1\infty})$
ϕ	angular coordinate
ω	angular velocity

Subscripts:

1	component 1, diffusing gas
2	component 2, main stream gas
∞	ambient conditions ($z \rightarrow \infty$)
c	convective
d	diffusive
dis	displacement
e	refers to entering temperature of coolant
m	momentum
t	thermal
w	conditions at surface ($z = 0$)

INTRODUCTION

E-438 The pioneering study of fluid flows in which there is mass addition or mass removal at a bounding surface was carried out by Prandtl in 1904. His attention was directed toward control of the boundary layer on aerodynamic bodies, an end which can be achieved by sucking fluid away through slots in the surface. Investigation of the problem of boundary-layer suction has continued up to the present. Results of these suction studies may also be applied when the mass removal comes about due to freezing (i.e., icing) at the surface.

In recent years, considerable interest has also been shown in mass addition to boundary layer flows, especially in connection with the cooling of turbine blades and the skins of high speed aero-vehicles. Such a cooling process, frequently termed transpiration, might utilize a porous surface through which a coolant, either a gas or liquid, is forced. In the case of a liquid coolant, evaporation would take place due to the hot boundary layer gases, and the latent heat of vaporization would thus be utilized. In an alternate technique of transpiration cooling, the surface of the vehicle would be fabricated of a material which would evaporate and hence cool the boundary layer.

From this discussion, it is clear that an attack on the problem of fluid injection or removal involves consideration of the flow velocities, the heat transfer, and the mass transfer. For boundary layer flows, a fundamental study of this type has been made by Hartnett and Eckert (ref. 1). As a logical first step, they examined the laminar boundary-layer equations for the case of a two component gas where the properties of the diffusing gas were identical to those of the free-stream fluid. The results of such an analysis can be applied to two-component systems in which the properties of the separate components are not too different (and, of course, to one component systems). But an even greater utility of such an analysis is that it indicates basic trends and behavior patterns.

In the present investigation, we turn to an altogether different physical configuration. The system to be studied, shown schematically in figure 1, is a

rotating disk immersed in a large body of otherwise quiescent fluid. Motions are induced within the fluid by the rotation of the disk. Mass transfer to or from the fluid may take place at the surface of the disk, either by direct injection or suction, or else by phase change. The rate of mass addition or removal is uniform at all points on the disk surface. Heat transfer may also take place due to a difference in temperature between the ambient fluid and the surface of the disk. As a first step, we study this problem by using the same assumptions about fluid properties as has been mentioned in connection with reference 1. The solutions and results thus obtained constitute a fundamental body of information which provides insight into behavior patterns and may also be of direct application to single component or to two-component gases. Consideration will be given here to the entire range of mass transfers, extending from large suction through small suction and injection to large injection.

A modest beginning on this problem has been made by Stuart (ref. 2). He confined his attentions to the effects of suction on the velocity distribution; heat and mass transfer were not considered. Most of his work was directed to large suction, with only a single case of moderate suction reported. No consideration was given to fluid injection.

ANALYSIS

The governing equations. - The velocity, temperature, and diffusion fields around a rotating disk are governed by the basic conservation principles: momentum, energy, and mass; and it is these which form the starting point of our study. The momentum principle is represented by the three Navier-Stokes equations, one for each coordinate direction; while energy conservation provides a fourth equation. For a multi-component gas, conservation of mass must be satisfied by the separate components. When there are two components, as is the case in the present analysis, mass conservation is fully expressed by a continuity equation for the mixture and a diffusion equation for one component.*

*This will guarantee that mass conservation is satisfied for the second component.

The mathematical statement of the conservation laws appropriate to a constant property, non-dissipative flow may be written in cylindrical coordinates as follows:

Momentum conservation

$$\rho \left(\frac{dV_r}{dt} - \frac{V_\phi^2}{r} \right) = - \frac{\partial p}{\partial r} + \mu \left(\nabla^2 V_r - \frac{2}{r^2} \frac{\partial V_\phi}{\partial \phi} - \frac{V_r}{r^2} \right) \quad (1)$$

$$\rho \left(\frac{dV_\phi}{dt} + \frac{V_r V_\phi}{r} \right) = - \frac{1}{r} \frac{\partial p}{\partial \phi} + \mu \left(\nabla^2 V_\phi + \frac{2}{r^2} \frac{\partial V_r}{\partial \phi} - \frac{V_\phi}{r^2} \right) \quad (2)$$

$$\rho \frac{dV_z}{dt} = - \frac{\partial p}{\partial z} + \mu \nabla^2 V_z \quad (3)$$

Energy conservation

$$\frac{dT}{dt} = \alpha \nabla^2 T \quad (4)$$

Mass conservation

$$\frac{1}{r} \frac{\partial}{\partial r} (r V_r) + \frac{1}{r} \frac{\partial V_\phi}{\partial \phi} + \frac{\partial V_z}{\partial z} = 0 \quad (5)$$

$$\frac{dW_1}{dt} = D \nabla^2 W_1 \quad (6)$$

where

$$\frac{d}{dt} = V_r \frac{\partial}{\partial r} + \frac{V_\phi}{r} \frac{\partial}{\partial \phi} + V_z \frac{\partial}{\partial z}$$

and

$$\nabla^2 = \frac{\partial^2}{\partial r^2} + \frac{1}{r} \frac{\partial}{\partial r} + \frac{\partial^2}{\partial z^2} + \frac{1}{r^2} \frac{\partial^2}{\partial \phi^2}$$

The symbols V_r, V_ϕ , and V_z represent the usual convective velocity components. So, the first five equations remain the same whether or not the gas diffusing out of (or into) the wall is the same as the main-stream component. So, within the framework of the constant property analysis, the velocity and temperature distributions are independent of the concentration field. Equation (6) is called the diffusion equation. It governs the distribution of the weight fraction W_1 , which is defined as the ratio of the partial density of component 1 to the total density. A similar definition applies to W_2 . Using the Gibbs-Dalton law, it follows that

$$\rho_1 + \rho_2 = \rho \quad \text{or} \quad W_1 + W_2 = 1 \quad (7)$$

In the derivation of equation (6), it has been assumed that the diffusion velocities are given by Fick's law (ref. 1), e.g.,

$$(v_z)_1 = - \frac{D}{W_1} \frac{\partial W_1}{\partial z}, \quad (v_z)_2 = - \frac{D}{W_2} \frac{\partial W_2}{\partial z}, \text{ etc.} \quad (8)$$

In this analysis, we will assign the subscript 1 to identify the component diffusing through the wall, while 2 will represent the other component (while would most likely be air).

The solution of the partial differential equations (1) through (6) would appear, at first glance, a too formidable task. Fortunately, we can draw on the experience of von Kármán (ref. 2), who successfully solved the velocity problem for an impermeable disk rotating in a single-component, incompressible fluid. Kármán used a similarity transform to reduce the partial differential equations of his problem to ordinary differential equations, which are easier to solve. Utilizing his idea, we introduce the following new variables

(a) new independent variable

$$\eta = z \left(\frac{\omega}{\nu} \right)^{1/2} \quad (9a)$$

(b) new dependent variables

$$\begin{aligned} F(\eta) &= \frac{V_r}{r\omega}, & G(\eta) &= \frac{V_\phi}{r\omega}, & H(\eta) &= \frac{V_z}{(\omega r)^{1/2}}, & P(\eta) &= \frac{p}{\mu\omega} \\ \theta(\eta) &= \frac{T - T_\infty}{T_w - T_\infty}, & \Phi(\eta) &= \frac{W_1 - W_{1\infty}}{W_{1w} - W_{1\infty}} \end{aligned} \quad (9b)$$

The similarity aspects of the transformation are linked to the supposition that (except for a simple stretching of V_r and V_ϕ) the velocity, temperature and concentration profiles do not change shape at different values of r . Also, the idea of angular symmetry has been invoked, i.e., $\partial/\partial\phi \equiv 0$.

Under the transformation, the conservation equations (1) through (6) become

$$F'' = HF' + F^2 - G^2 \quad (1a)$$

$$G'' = HG' + 2FG \quad (2a)$$

$$P' = H'' - HH' \quad (3a)$$

$$\theta'' = (Pr)H\theta' \quad (4a)$$

$$H' = -2F \quad (5a)$$

$$\Phi'' = (Sc)H\Phi' \quad (6a)$$

where Pr and Sc respectively represent the Prandtl and Schmidt numbers. The primes denote differentiation with respect to η . Although the transformation has provided a set of ordinary differential equations, a closed form solution is still not within our grasp, and numerical techniques must be used. For computational convenience, it is desirable to eliminate F from equations (1a), (2a), and (5a), giving

$$H''' = HH'' - (H')^2/2 + 2G^2 \quad (10)$$

$$G'' = HG' - H'G \quad (11)$$

Simultaneous solution of these will yield H and G . Then, with a solution for H at our disposal, equations (4a) and (6a) may be attacked. If $Pr = Sc$ and if the boundary conditions coincide, then equations (4a) and (6a) have identical solutions. The pressure distribution is somewhat incidental to the problem and no further attention will be given to equation (3a).

Boundary conditions. - The conservation equations give, within the framework of the simplifying assumptions, a complete description of the physical occurrences within the fluid. But, to complete the statement of the problem, it still remains to specify the boundary conditions.

For the velocity problem, it will be supposed that the no-slip condition of viscous flow continues to apply at the surface of the disk. Further, the convective velocity V_{zw} normal to the disk surface specifies the mass injection or withdrawal. Far from the disk surface, all fluid velocities must vanish aside from the induced axial component.

For the energy and diffusion equations, the temperature and weight fraction must, by continuity considerations, respectively equal T_w and W_{1w} at the disk surface. At large distances from the disk, $T \rightarrow T_\infty$ and $W_1 \rightarrow W_{1\infty}$.

A formal statement of these conditions is:

$$\left. \begin{array}{l} V_r = 0 \\ V_\phi = r\omega \\ V_z = V_{zw} \\ T = T_w \\ W = W_{1w} \end{array} \right\} z=0 \quad \left. \begin{array}{l} V_r \rightarrow 0 \\ V_\phi \rightarrow 0 \\ T \rightarrow T_\infty \\ W_1 \rightarrow W_{1\infty} \end{array} \right\} z \rightarrow \infty \quad (12a)$$

In terms of the transformed variables, equation (12a) becomes

$$\left. \begin{array}{l} H = H_w \\ H' = 0 \\ G = 1 \\ \theta = 1 \\ \Phi = 1 \end{array} \right\} \eta=0 \quad \left. \begin{array}{l} H' \rightarrow 0 \\ G \rightarrow 0 \\ \theta \rightarrow 0 \\ \Phi \rightarrow 0 \end{array} \right\} \eta \rightarrow \infty \quad (12b)$$

where H_w represents the dimensionless velocity normal to the disk surface. Positive values of H_w denote fluid injection, while negative values denote suction (i.e., mass withdrawal).

Up to this point, we have been at liberty to assign whatever values we please to V_{zw} , W_{1w} , $W_{1\infty}$, etc. Solutions of the conservation equations can be obtained for any choices of these parameters. However, as pointed out in reference 1, there are a number of important situations where there is an added physical constraint which provides a relationship between V_{zw} and the boundary values of W_1 . The temperature boundary values may also be interrelated through an additional physical constraint. Illustrations of these constraints and relationships will be given when the heat transfer and mass transfer results are discussed.

Solutions. - The velocity problem is governed by the differential equations (10) and (11) subject to the boundary conditions (12b). By inspection of these conditions, it is seen that solutions cannot be obtained until numerical values of the dimensionless mass-transfer velocity H_w are prescribed. For a large number of values of H_w ranging from -4 to +5 as listed in table I, solutions of equations (10) and (11) have been carried out on an IBM 653 electronic computer utilizing the numerical techniques of reference 3. The method is a forward integration procedure and the critical quantities which define a solution are the derivatives $H''(0)$ and $G'(0)$ which are needed to start the numerical computation. A listing of these starting values is given in table I. It will later be shown that the $H''(0)$ and $G'(0)$ are also of direct application in shear stress computations. For large positive values of H_w , the limitations of a computing machine which uses eight significant figures were keenly felt. The information listed in table I for $H_w = 4$ and 5 is believed to be correct to at least the number of places given, but the corresponding solutions do not accurately satisfy the boundary conditions at large η .

Turning to the temperature and diffusion equations ((4a) and (6a), respectively), solutions were carried out for $Pr = Sc = 0.7$. There was, thus, no mathematical distinction between the equations. The needed input data for $H(\eta)$ was supplied by the previously mentioned solutions of equations (10) and (11). Since $H(\eta)$ is a function of H_w , so too are $\theta(\eta)$ and $\phi(\eta)$. The values of $\theta'(0) = \phi'(0)$ obtained from

these solutions are listed in table I.* These are the starting values in our forward integration procedure and, as will be shown later, are directly related to the heat and mass-transfer coefficients.

For large suction velocities (large negative values of H_w), certain simple asymptotic solutions can be obtained. These will be discussed in a later section where their motivation is clear.

RESULTS

Velocity distributions. - Insight into the physical occurrences within the flow field can be obtained by study of the velocity profiles. Inasmuch as space limitations preclude presentation of velocity data for all the cases listed in table I, we must content ourselves here with graphing the results for representative situations.

We turn our attention first to the distribution of the axial velocity V_z . Positive values indicate an outflow toward the free stream; while negative values represent an inflow from the free stream toward the disk. The distribution of V_z plotted as a function of distance normal to the disk is presented in figure 2 for representative values of the dimensionless injection (or suction) velocity H_w . Consider first the case of the impermeable surface, $H_w = 0$. The rotating disk acts like a fan, drawing fluid axially inward from the surroundings toward the disk surface. However, because the surface is solid, the inflowing fluid finds its path blocked, and it must reroute into a radial direction where there is no obstruction. So on figure 2, we see that the negative velocity of inflow, starting from its largest value at large z , decreases steadily as we approach the disk (decreasing z) due to fluid escape into the radial direction. Now, consider the application of a suction at the disk surface (i.e., $H_w < 0$). Then, besides the fan-like pumping of the rotating disk, there is the additional pumping due to the suction. So, the quantity of fluid drawn in from the surroundings increases; or in terms of figure 2, the magnitude of $V_{z\infty}$ increases. Now, the inflowing fluid has two possible paths. It may continue

*Solutions of the θ equation were not attempted for $H_w = 4$ and 5 because the available values of $H(\eta)$ were not sufficiently accurate to serve as input data.

E-438

its inflow through the suction holes of the disk, or, it may reroute into the radial direction. The path chosen will, of course, be that of least resistance. As the wall suction increases, escape through the wall becomes easier and easier. So, with H_w becoming increasingly negative, more and more of the inflow goes directly into the porous disk. As a consequence, V_z tends to become almost constant with z . Next, consider the case of blowing (injection) at the disk surface. In this instance, the fluid drawn in by the fan action of the disk finds itself actively retarded by the outflowing stream of injected fluid. The greater the blowing velocity, the more strongly is the inflow opposed. The result is a decrease in the magnitude of $V_{z\infty}$ with increasing H_w . There is, in a real sense, a battle between the two streams; and as H_w increases, the outflow penetrates to greater distances from the disk surface. As a consequence, the cross-over point between positive and negative V_z is pushed farther outward.

These events are reflected by the radial velocity distribution. Representative profiles are given in figure 3. Since the radial velocity is zero both at the disk surface and in the ambient fluid, there must be a maximum value somewhere between. The maximum is positive since the radial flow is always outward along the disk. For the impermeable disk ($H_w = 0$), all the axial inflow is ultimately diverted into radial flow. With increasing suction, more and more of the inflowing fluid passes directly into the porous wall; so, the radial velocities decrease as H_w becomes more negative. Further, since less fluid makes the turn from axial to radial flow, it can be accomplished closer to the surface, and hence $(V_r)_{\max}$ occurs at smaller z .
($H_w > 0$)
When blowing is applied, the radial velocity must carry away not only the incoming axial flow, but also the injected fluid. So, the general level of the radial velocity is raised with increased blowing. But, the finer details bear further discussion. First of all, with increasing H_w , the injected stream might be expected to sustain its axial motion to greater distances from the wall. So, near the wall, the radial velocity (which is fed by diverted axial flow) might be expected to decrease as the blowing increases. This is substantiated by comparing the curves for $H_w = 1$ and

$H_w = 3$ at small values of z . But, as shown in the inset of figure 3, quite the contrary is true at very small values of blowing: the velocities near the wall increases with increasing H_w . A reasonable explanation is that for small blowing, the injected stream is not strong enough to maintain its axial velocity and is diverted immediately into a radial flow, thereby augmenting V_r near the wall. An alternate demonstration of this interesting occurrence near the disk surface may be given as follows: For very small values of z , we can write

$$V_r = \left(\frac{\partial V_r}{\partial z} \right)_w z \quad \text{or} \quad \frac{V_r}{r\omega} = [-H''(0)] \eta$$

So, the radial velocity immediately adjacent to the disk is proportional to $H''(0)$. From figure 6, where $[-H''(0)]$ is plotted against H_w , we see that V_r (at small η) increases with increased blowing from $H_w = 0$ to about 0.3, and, thereafter decreases.

The tangential velocity component V_ϕ is directly driven through the action of viscosity by the rotation of the disk. It thus shares a common characteristic with the boundary layer forward flow velocity V_x , which is also impelled by an external driver - the free stream. The effect of fluid injection or withdrawal on the tangential component V_ϕ is remarkably similar to the well-established effects on V_x . Figure 4 shows the distribution of V_ϕ^* as a function of distance normal to the disk for representative values of the mass-transfer velocity H_w . It is easily seen that fluid injection ($H_w > 0$) gives rise to the familiar S-shaped (inflection point) profiles, the effect becoming more pronounced with increased blowing. Since the presence of an inflection point is known to destabilize a laminar boundary layer, it would be expected that transition to turbulence would occur at lower Reynolds numbers as the blowing becomes stronger. The velocity profile becomes progressively flatter near the wall, suggesting the well-known "blow-off" phenomenon in which the viscous layer is lifted off the surface. Blow-off is characterized by the condition

$$(dV_\phi/d\eta)_w = 0 \quad \text{or} \quad G'(0) = 0$$

*The similarity between V_ϕ and V_x is best seen by turning figure 4 top to bottom.

In the plot of $G'(0)$ against the blowing parameter (fig. 6), it is seen that $G'(0)$ is indeed approaching zero with increasing H_w , but we were unable to find the exact blow-off point because of the limitation of an eight-place computer. Returning to figure 4, it may be observed that suction ($H_w > 0$) has its usual effect of thinning the viscous layer, thereby increasing the stability of the laminar flow.

Temperature and concentration distributions. - The distribution of the dimensionless temperature and concentration as a function of distance from the disk is given in figure 5 for representative values of H_w . Since we have selected $Pr = Sc$, the same curves and a similar discussion applies for both θ and ϕ ; and for brevity's sake, we will only make reference to the temperature. The action of fluid injection ($H_w > 0$) is to fill the space immediately adjacent to the disk with fluid having nearly the same temperature as that of the disk. As the blowing becomes stronger, so then does the blanket extend to greater distances from the surface. As shown on figure 5, these effects are manifested by the progressive flattening of the temperature profile adjacent to the disk. Thus, the injected fluid forms an effective insulating layer, decreasing the heat transfer from the disk (fig. 7). Suction, on the other hand, serves the function of bringing large quantities of ambient fluid into the immediate neighborhood of the disk surface. As a consequence of the increased heat consuming ability of this augment flow, the temperature drops quickly as we proceed away from the disk. The presence of fluid at near-ambient temperature close to the surface increases the heat transfer (fig. 7).

Shear stress and shaft torque. - The action of viscosity in the fluid adjacent to the disk tends to set-up a tangential shear stress which opposes the rotation of the disk. As a consequence, it is necessary to provide torque at the shaft to maintain a steady rotation. To find the tangential stress τ_ϕ , we apply the Newtonian shear formula

$$\tau_\phi = \mu(\partial V_\phi / \partial z)_w \quad (13a)$$

In terms of the variables of the analysis, this expression becomes

$$\tau_\phi / \rho r (\nu \omega^3)^{1/2} = G'(0) \quad (13b)$$

The shaft torque M required to overcome the shear on one side of a rotating disk is

$$M = - \int_0^{r_0} r \tau_{\varphi} 2\pi r dr \quad (14a)$$

where r_0 is the disk radius. Utilizing equation (13b), there is obtained

$$2M/\pi r_0^4 \rho (\omega^3)^{1/2} = -G'(0) \quad (14b)$$

So, both the tangential shear τ_{φ} and the torque M are proportional to the slope $G'(0)$ of the tangential velocity profile which has been listed in table I. The torque and tangential shear results are plotted on figure 6 as a function of the mass transfer velocity H_w . The effect of blowing is to decrease the tangential shear and the torque requirements. These quantities take on zero values at the blow-off point, but computing limitations prevented the determination of this condition. The effects of suction are opposite to those of blowing. These findings reflect the changes in tangential velocity profile as previously discussed and are qualitatively similar to the effects of mass transfer on the skin friction in a boundary layer flow.

There is also a surface shear stress τ_r in the radial direction which, practically speaking, is of lesser importance than is the tangential stress. Again, using the Newton shear relations and then introducing the variables of the analysis, there is obtained

$$\tau_r = \mu \left(\frac{\partial v_r}{\partial z} \right)_w \quad \text{or} \quad \tau_r / \rho r (\omega^3)^{1/2} = -\frac{1}{2} H''(0) \quad (15)$$

This dimensionless shear stress has been plotted on figure 6. A maximum value, which has already been discussed in relation to the velocity profiles, is achieved at about $H_w = 0.3$.

Heat transfer and surface temperature. - The heat transfer from the disk surface to the fluid is computed by application of Fourier's law

$$q = -k (\partial T / \partial z)_w$$

Introducing the transformed variables, the expression for q becomes

$$q = -k (T_w - T_{\infty}) \left(\frac{\omega}{\nu} \right)^{1/2} \theta'(0) \quad (16)$$

It is customary to rephrase the heat transfer results in terms of a heat transfer coefficient and a Nusselt number, which are defined as follows

$$h \equiv \frac{q}{T_w - T_\infty}, \quad Nu = \frac{h(\nu/\omega)^{1/2}}{k} \quad (17)$$

where $(\nu/\omega)^{1/2}$ plays the role of a characteristic length. With this, equation (16) becomes

$$Nu = -\theta'(0) \quad (18)$$

The Nusselt number results are presented in figure 7 as a function of the dimensionless mass-transfer velocity H_w . As has already been noted, the effect of fluid injection ($H_w > 0$) is to significantly decrease the heat transfer (and hence, the Nusselt number) by blanketing the surface with fluid whose temperature is close to T_w . Suction has an opposite effect on the heat transfer, since fluid at near-ambient temperature is brought to the neighborhood of the disk surface.

With these heat-transfer results at our disposal, we may proceed to make application to specific situations. Consider the situation of mass transfer cooling (from a supply tank) by a gas. The coolant gas enters the porous disk / at a temperature T_e and is heated in its course of flow through the wall. The flow passages are so arranged that the coolant emerges at a temperature T_w , equal to that of the disk surface. It is of interest to determine how T_w is related to the other parameters of the problem. In the absence of heat losses by conduction and radiation, an energy balance on a control volume spanning the thickness of the porous wall yields

$$m_1 c_p (T_w - T_e) = h(T_\infty - T_w) \quad (19a)$$

The left hand side is the energy absorbed by the coolant gas, while the right side is the heat transferred to the disk surface from the ambient fluid. Borrowing the result that $m_1 = \rho V_{zw}$ from equation (28) and introducing the definitions of the Nusselt and Prandtl numbers, equation (19a) may be rephrased as

$$\frac{T_w - T_e}{T_\infty - T_w} = \frac{Nu}{Pr H_w} \quad (19b)$$

Suppose that the entering coolant temperature T_e and the free-stream condition T_∞ are known. Further, when the blowing rate H_w is presented, the value of Nu

may be read from figure 7. Hence, equation (19b) permits the determination of the temperature T_w of the disk surface as follows

$$T_w = \frac{T_\infty \left(\frac{Nu}{PrH_w} \right) + T_e}{1 + \frac{Nu}{PrH_w}} \quad (19c)$$

It is clear from equation (19c) that increased blowing causes the wall temperature T_w to approach more and more closely to T_e . As an alternative, equation (19b) can be solved to provide either the blowing velocity or the coolant temperature needed to maintain a given T_w .

Equations (19b) or (19c) illustrate the statement, made in discussing the boundary conditions, that there are important applications in which all of the boundary temperatures cannot be prescribed independently.

Additional examples showing the application of the Nusselt number results are given in reference 1.

Mass transfer. - The previous derivation of the heat-transfer coefficient and Nusselt number can be duplicated for diffusion. For component 1, the mass transfer at the disk surface by diffusion alone is given by Fick's law (8) as

$$m_{1d} = \rho_{1w} \left(- \frac{D}{W_1} \frac{\partial W_1}{\partial z} \right)_w = -\rho D \left(\frac{\partial W_1}{\partial z} \right)_w \quad (20)$$

Now, defining a diffusional transfer coefficient and diffusional Nusselt number as

$$h_d \equiv \frac{m_{1d}}{(W_{1w} - W_{1\infty})}, \quad Nu_d \equiv \frac{h_d (\nu/\omega)^{1/2}}{\rho D} \quad (21)$$

and introducing the variables of the analysis, there is obtained

$$Nu_d = [-\phi'(0)] \quad (22)$$

This is identical to the result for the heat transfer Nusselt number which has already been plotted on figure 7.

Now, the total mass flow of component 1 at the disk surface is due to both diffusion (subscript d) and convection (subscript c). So, we write

$$m_1 = m_{1d} + m_{1c} \quad (23a)$$

Convection contributes an amount $\rho_{1w} V_{zw}$, while the diffusional contribution can be computed from equations (21) and (22). Introducing this information into (23a) and

rearranging, we find

$$\frac{m_1}{\rho(\omega v)^{1/2}} = W_{1w} H_w + \frac{Nu_d}{Sc} (W_{1w} - W_{1\infty}) \quad (23b)$$

Proceeding in a similar way for component 2, and using the fact that $W_1 + W_2 = 1$, there is obtained

$$\frac{m_2}{\rho(\omega v)^{1/2}} = (1 - W_{1w}) H_w - \frac{Nu_d}{Sc} (W_{1w} - W_{1\infty}) \quad (24)$$

The combined mass transfer of both components at the surface is given by

$$m = m_1 + m_2 \quad (25a)$$

Adding equations (23b) and (24), we get

$$\frac{m}{\rho(\omega v)^{1/2}} = H_w \quad \text{or} \quad m = \rho V_{zw} \quad (25b)$$

So, as expected, it is the convective velocity V_{zw} which transports mass for the combined flow.

Now, we turn to applications. In the discussion of the boundary conditions, it was noted that in many situations there is a physical constraint which relates the velocity V_{zw} and the mass fractions W_{1w} and $W_{1\infty}$. The constraint which is most frequently encountered is the condition of no net mass flow of component 2 (e.g., the main stream component) into or out of the disk surface. When the mass addition or removal of component 1 is due to evaporation, sublimation, or freezing, it is clear that component 2 will be unable to enter or leave the surface. In the case of a coolant gas passing through a porous wall, the condition of no net mass flow of component 2 into the wall is still correct, provided that the coolant gas in the supply tank is pure component 2.* Proceeding to the mathematical formulation of this constraint, we observe that

$$m_2 = 0 = m_{2d} + m_{2c}$$

So, to make $m_2 = 0$, the diffusive flow of component 2 into the wall is balanced by a convective outflow. Utilizing equation (24) with $m_2 = 0$, we get

$$\frac{H_w(Sc)}{Nu_d} = \frac{W_{1w} - W_{1\infty}}{1 - W_{1w}} \quad (26)$$

*Additional discussion will be found in reference 1.

or, in terms of physical variables

$$V_{zw} = - \frac{D}{1 - W_{1w}} \left(\frac{\partial W_1}{\partial z} \right)_w \quad (27)$$

For a given H_w , Nu_d is known. So, equation (26) expresses the fact that for no net mass flow of component 2 into the wall, only two of the quantities W_{1w} , $W_{1\infty}$, and H_w may be selected independently. When $m_2 = 0$, it follows from equations (25a) and (25b) that

$$m_1 = m = \rho V_{zw} \quad (28)$$

An important special case of mass transfer cooling occurs when the mass fraction of the coolant gas is zero in the free stream, i.e., $W_{1\infty} = 0$. Then, equation (26) becomes

$$W_{1w} = \frac{1}{1 + Nu_d/H_w(Sc)} \quad (29)$$

So, W_{1w} is fixed when H_w is specified and vice-versa. Utilizing the Nusselt number results of figure 7, we have plotted the variation of W_{1w} with H_w on figure 8. It is seen that the coolant mass fraction (W_{1w}) at the wall increases rapidly with blowing rate and is greater than 0.95 for $H_w > 1.3$.

Thickness of viscous and thermal layers; ambient inflow. - Our solutions show that the significant velocity and temperature variations in the fluid are confined to the region adjacent to the disk. To define the thickness of these layers, we use certain standard measures.

The first of these is the displacement thickness. Inasmuch as we are dealing with a three-dimensional problem, the initial thought might be to evaluate separate displacement thicknesses for both the radial and tangential directions. However, since the radial flow is zero both at the disk surface and at infinity, a radial displacement thickness would have very little meaning. Then, for the tangential direction, we define a displacement thickness as

$$\delta_{dis} = \int_0^\infty \frac{V_\phi}{r\omega} dz \quad \text{or} \quad \delta_{dis}/(\nu/\omega)^{1/2} = \int_0^\infty G d\eta \quad (30)$$

In physical terms, δ_{dis} gives the thickness of a fictitious layer of fluid which is rotating at a uniform tangential velocity $r\omega$ and is carrying a tangential mass

flow equal to that carried by the actual tangential velocity distribution. Values of the displacement thickness are given in table I. It is seen that suction appreciably reduces the thickness of the viscous layer, while blowing increases the thickness.

A momentum thickness for flow about a rotating disk has been defined by Stuart (2) as

$$\delta_m / (\nu/\omega)^{1/2} \equiv \int_0^\infty G(1 - G) dy \quad (31)$$

While this expression has a form similar to that for the boundary-layer momentum thickness, we are unable to give it a clear physical meaning. Values of δ_m are listed in table I and show qualitative trends similar to these for δ_{dis} .

As a measure of the extent of the thermal layer, we may introduce a thermal thickness based on the temperature excess $T - T_\infty$ above the ambient fluid. Then,

$$\delta_t \equiv \int_0^\infty \frac{T - T_\infty}{T_w - T_\infty} dy \quad \text{or} \quad \delta_t / (\nu/\omega)^{1/2} = \int_0^\infty \theta d\eta \quad (32)$$

Physically speaking, δ_t is the thickness of a fictitious fluid layer at temperature T_w whose integrated temperature excess over T_∞ is identical with that of the actual temperature distribution. Numerical values of the thermal thickness are listed in table I as a function of the mass transfer velocity H_w . With blowing, the thermal thickness increases; while with suction, it decreases.

The extent of the thermal layer is sometimes characterized by a convection thickness (ref. 9, pp. 118-119). In reference 9, the definition of such a thickness was motivated by the results of an over-all energy balance. Setting up such a balance for the present problem, we find

$$\frac{Nu}{Pr} = -H_w - \int_0^\infty H' \theta d\eta \quad (33)$$

The integral represents the convection of energy in the radial direction. So, in analogy to previous work, we define

$$\delta_c / (\nu/\omega)^{1/2} \equiv - \int_0^\infty H' \theta d\eta = \frac{Nu}{Pr} + H_w \quad (34)$$

The convective thickness can be evaluated using figure 7 or table I, since $Nu = -\theta'(0)$. It may easily be verified that δ_c increases with blowing and decreases with suction.

It may also be of interest to know the quantity of ambient fluid which is drawn inward toward the rotating disk. The inflow velocity of the ambient fluid is $V_{z\infty}$ and its dimensionless counterpart is H_∞ . A listing of H_∞ values is given in table I. As expected on the basis of previous discussion, H_∞ increases with suction and decreases with blowing. The information given in table I may also be to compute the radial flow. Imagine a cylindrical control surface of radius r extending from the disk surface to the ambient fluid. Then, the flow passing through this cylindrical surface is

$$\text{Radial flow} = \rho \pi r^2 [V_{zw} - V_{z\infty}] = \rho \pi r^2 (\omega v)^{1/2} [H_w - H_\infty]$$

For large suction, table I shows that $H_w - H_\infty$ is very small, indicating a small radial flow. The effect of blowing is to increase the radial flow.

ASYMPTOTIC SOLUTIONS

For large suction (i.e., large negative values of H_w), it is possible to find simple asymptotic solutions of the governing equations. The key to the simplification is the fact, graphically displayed on figure 2, that the axial velocity V_z is essentially constant throughout the flow when the suction is strong. In terms of the dimensionless variables of the analysis, this means that H is essentially independent of η for a fixed value of H_w . With this, equations (4a) and (6a) become

$$\theta'' = (Pr)H_w\theta' \quad \text{and} \quad \phi'' = (Sc)H_w\phi' \quad (34a)$$

A solution satisfying the boundary conditions is

$$\theta = e^{(Pr)H_w\eta}, \quad \phi = e^{(Sc)H_w\eta} \quad (34b)$$

from which it follows that

$$\theta'(0) = (Pr)H_w, \quad \phi'(0) = (Sc)H_w \quad (34c)$$

For $Pr = Sc = 0.7$ and $H_w = -4.0$, equation (34c) predicts that $\theta'(0) = \phi'(0) = -2.8$. This is in excellent agreement with the value -2.802 which appears in table I.

Proceeding in the same manner, it is easy to show that solution of equation (11) for G is

$$G = e^{H_w \eta}, \quad G'(0) = H_w \quad (35)$$

The $G'(0)$ prediction of equation (35) for $H_w = -4$ is very close to the value 4.005 given in table I.

Continuing, we may use equation (10) to predict values of $H''(0)$. Noting that $(H')^2/2$ is smaller than the other terms, we integrate between limits of $\eta = 0$ and $\eta = \infty$ and get

$$H''(0) = \frac{1}{H_w} \quad (36)$$

For $H_w = -4$, equation (36) gives $H''(0) = -0.25$, which is in excellent agreement with the value of -0.2495 of table I.

With these results, it is easy to derive that the thickness parameters take the following form for large negative values of H_w

$$\frac{\delta_{dis}}{(\nu/\omega)^{1/2}} = -\frac{1}{H_w}, \quad \frac{\delta_m}{(\nu/\omega)^{1/2}} = -\frac{1}{2H_w}, \quad \frac{\delta_t}{(\nu/\omega)^{1/2}} = -\frac{1}{(Pr)H_w}, \quad \delta_c = 0 \quad (37)$$

REFERENCES

1. Hartnett, J. P., and Eckert, E. R. G.: Mass-Transfer Cooling in a Laminar Boundary Layer with Constant Fluid Properties. Trans. ASME, vol. 79, 1957, pp. 247-254.
2. Stuart, J. T.: On the Effects of Uniform Suction on the Steady Flow Due to a Rotating Disk. Quart. Jour. Mech. and Math., Vol. 7, 1954, pp. 446-457.
3. Gregg, J. L.: A General Purpose IBM 653 Routine for the Solution of Simultaneous Ordinary Differential Equations. IBM 650 Scientific Computation Seminar, Endicott, N.Y., October 1957.
4. Eckert, E. R. G.: Introduction to the Transfer of Heat and Mass. McGraw-Hill Book Co., New York, N.Y., 1949.

TABLE I. - SOME IMPORTANT PROPERTIES OF THE SOLUTIONS

H_w	$-H''(0)$	$-G'(0)$	$-\theta'(0) = -\phi'(0)$	$\frac{\delta_{dis}}{(\nu/\omega)^{1/2}}$	$\frac{\delta_m}{(\nu/\omega)^{1/2}}$	$\frac{\delta_t}{(\nu/\omega)^{1/2}}$	$-\frac{V_{z\infty}}{(\nu\omega)^{1/2}}$
-4	0.2495	4.005	2.802	0.2496	0.1248	0.3566	4.008
-3	.3312	3.012	2.106	.3315	.1657	.4741	3.018
-2.5	.3947	2.521	1.759	.3957	.1977	.5663	2.531
-2	.4848	2.039	1.418	.4875	.2434	.6995	2.058
-1.5	.6136	1.580	1.087	.6226	.3100	.8999	1.620
-1.2	.7104	1.328	.8998	.7300	.3622	1.066	1.391
-.8	.8463	1.036	.6730	.9000	.4423	1.348	1.150
-.4	.9576	.8016	.4798	1.085	.5240	1.698	.9872
-.2	.9956	.7033	.3969	1.178	.5625	1.895	.9298
-.08	1.012	.6497	.3515	1.234	.5846	2.020	.9014
0	1.020	.6159	.3231	1.271	.5989	2.106	.8845
.06	1.025	.5916	.3028	1.299	.6094	2.170	.8728
.1	1.028	.5758	.2897	1.318	.6163	2.214	.8654
.3	1.034	.5022	.2295	1.412	.6496	2.448	.8331
.5	1.029	.4364	.1782	1.506	.6811	2.685	.8070
.6	1.023	.4063	.1557	1.554	.6962	2.814	.7960
.7	1.015	.3779	.1353	1.602	.7111	2.941	.7859
.8	1.004	.3511	.1167	1.650	.7255	3.076	.7766
1	.9790	.3022	.08539	1.749	.7536	3.345	.7605
1.6	.8758	.1885	.02806	2.061	.8338	4.187	.7251
2	.7979	.1360	.01140	2.286	.8853	4.765	.7065
3	.6183	.06029	.0006204	2.902	1.017	6.214	.6707
4	.486	.0289					
5	.395	.0155					

E-438

E-438

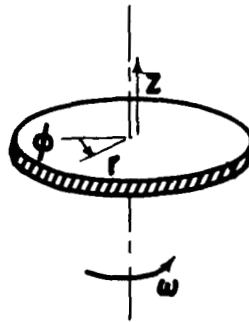


Fig. 1 - Physical model and coordinates.

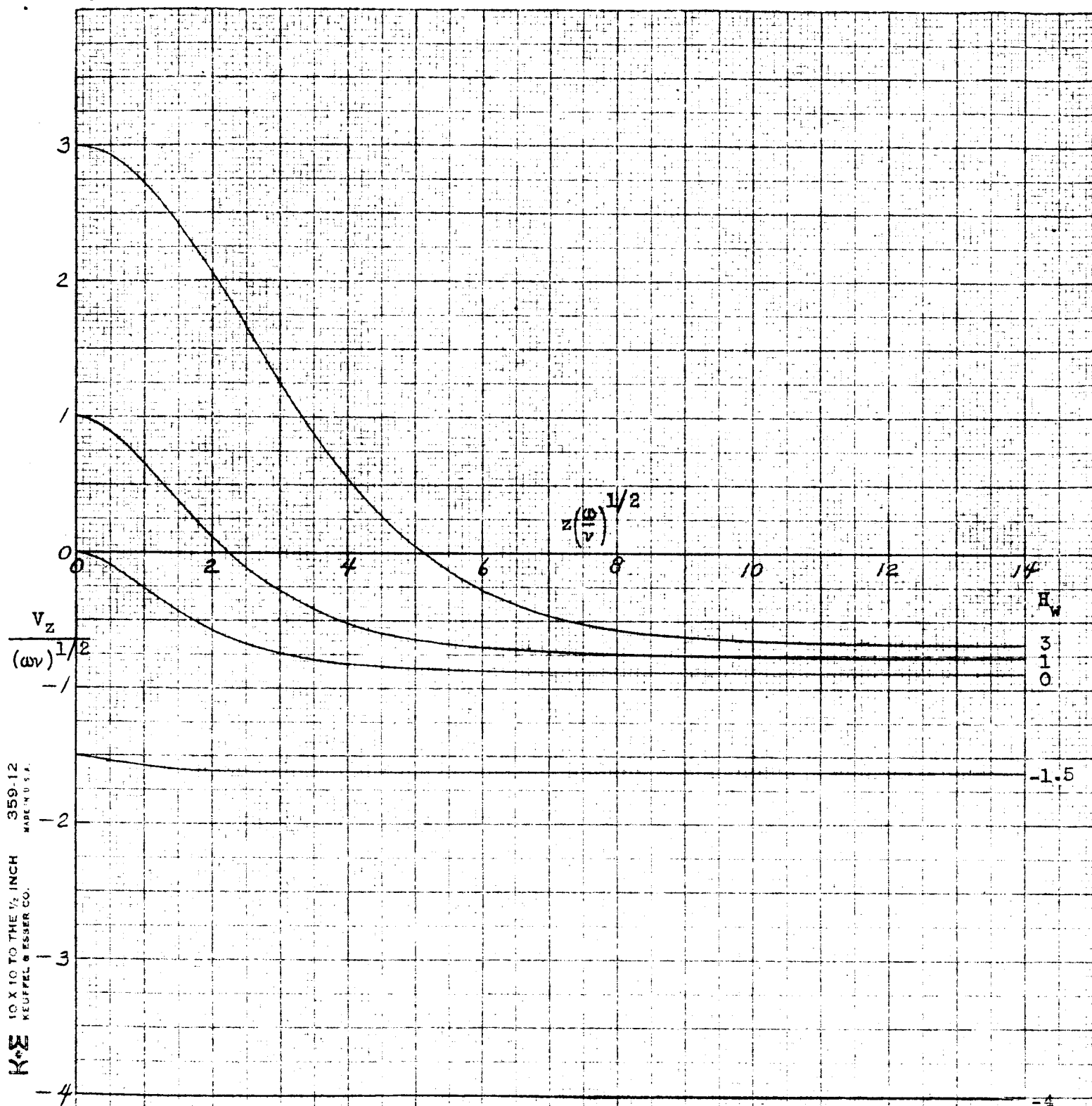


Figure 2. - Representative axial velocity distributions.

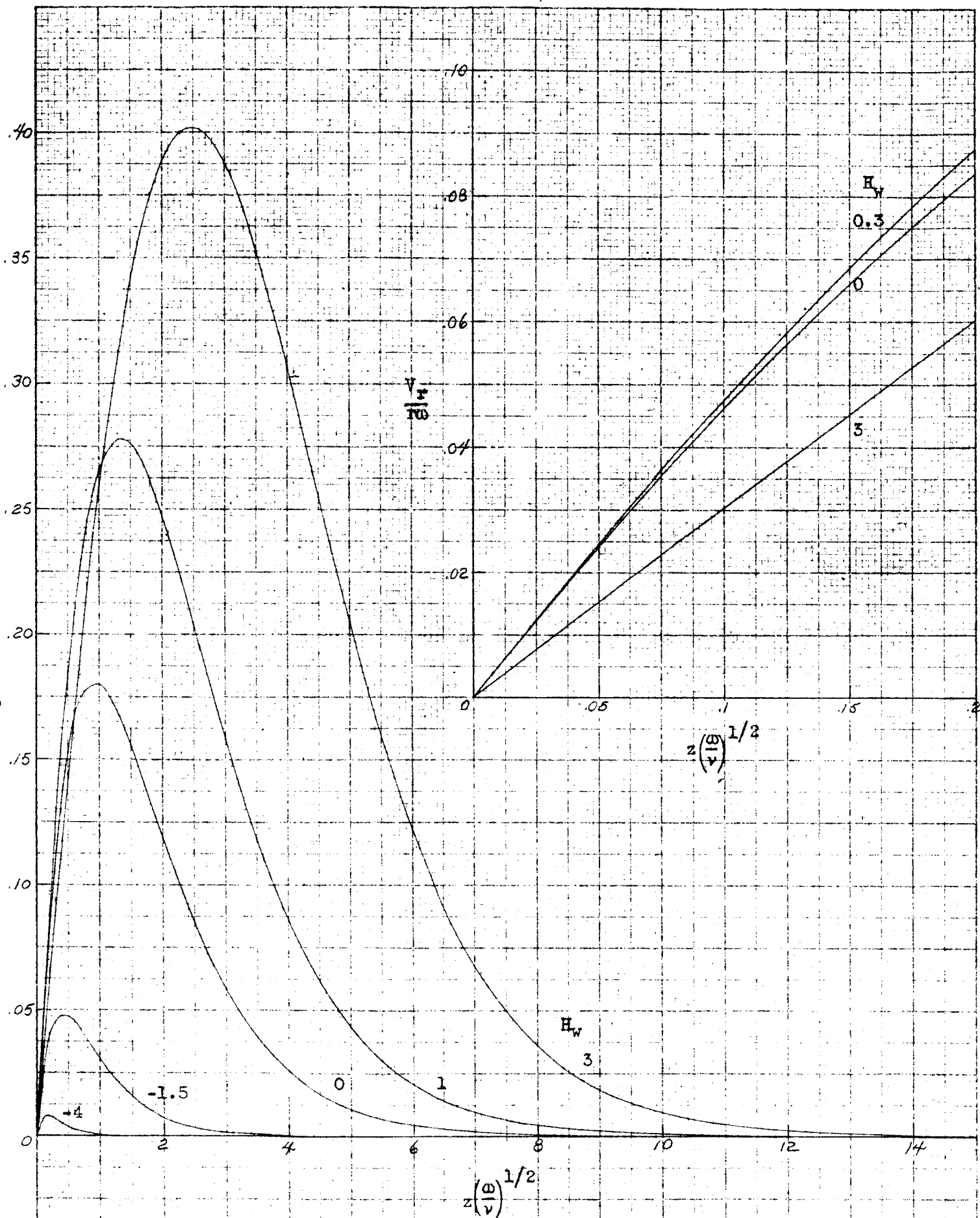
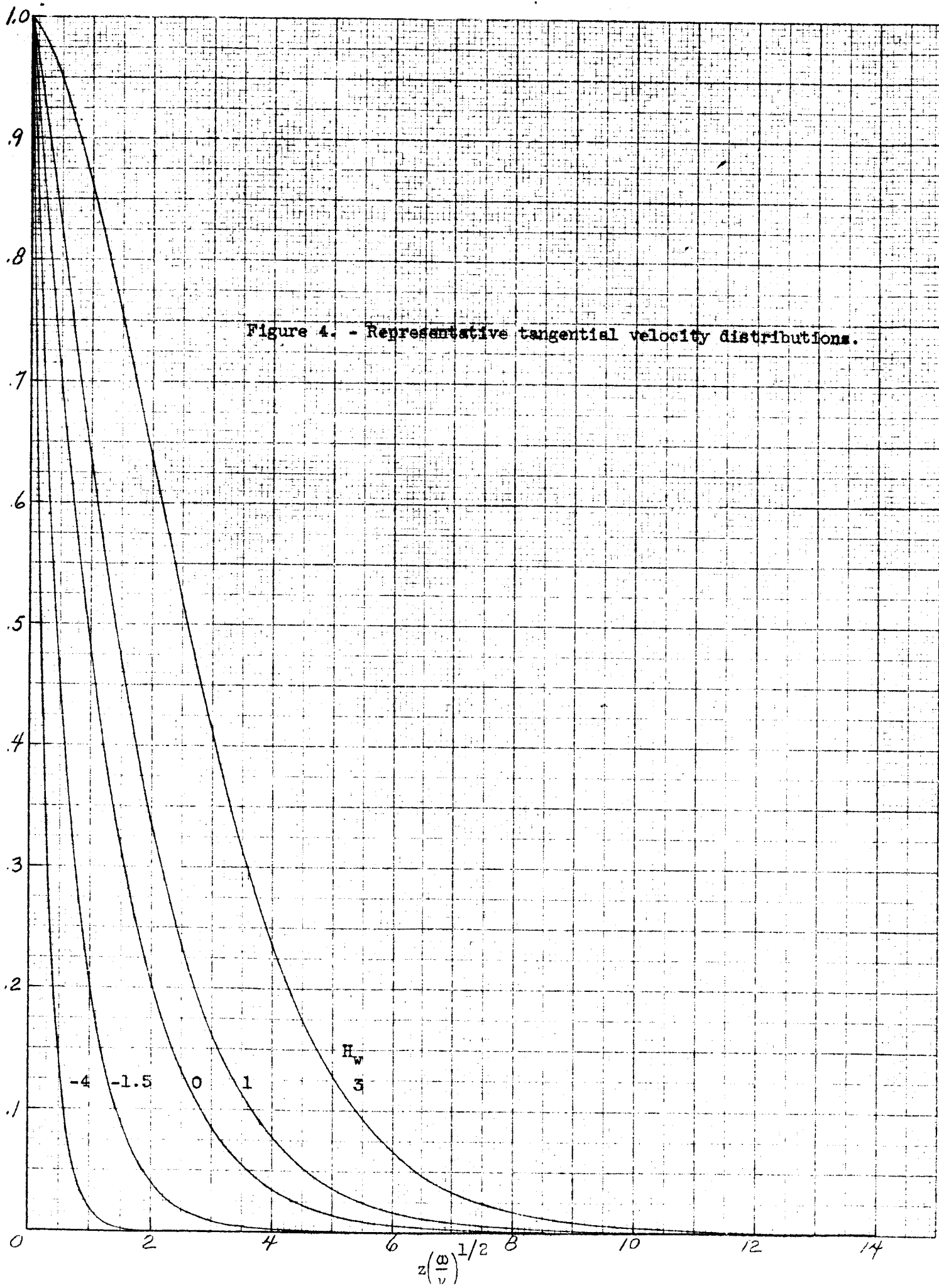


Figure 3. - Representative radial velocity distributions.

Figure 4. - Representative tangential velocity distributions.

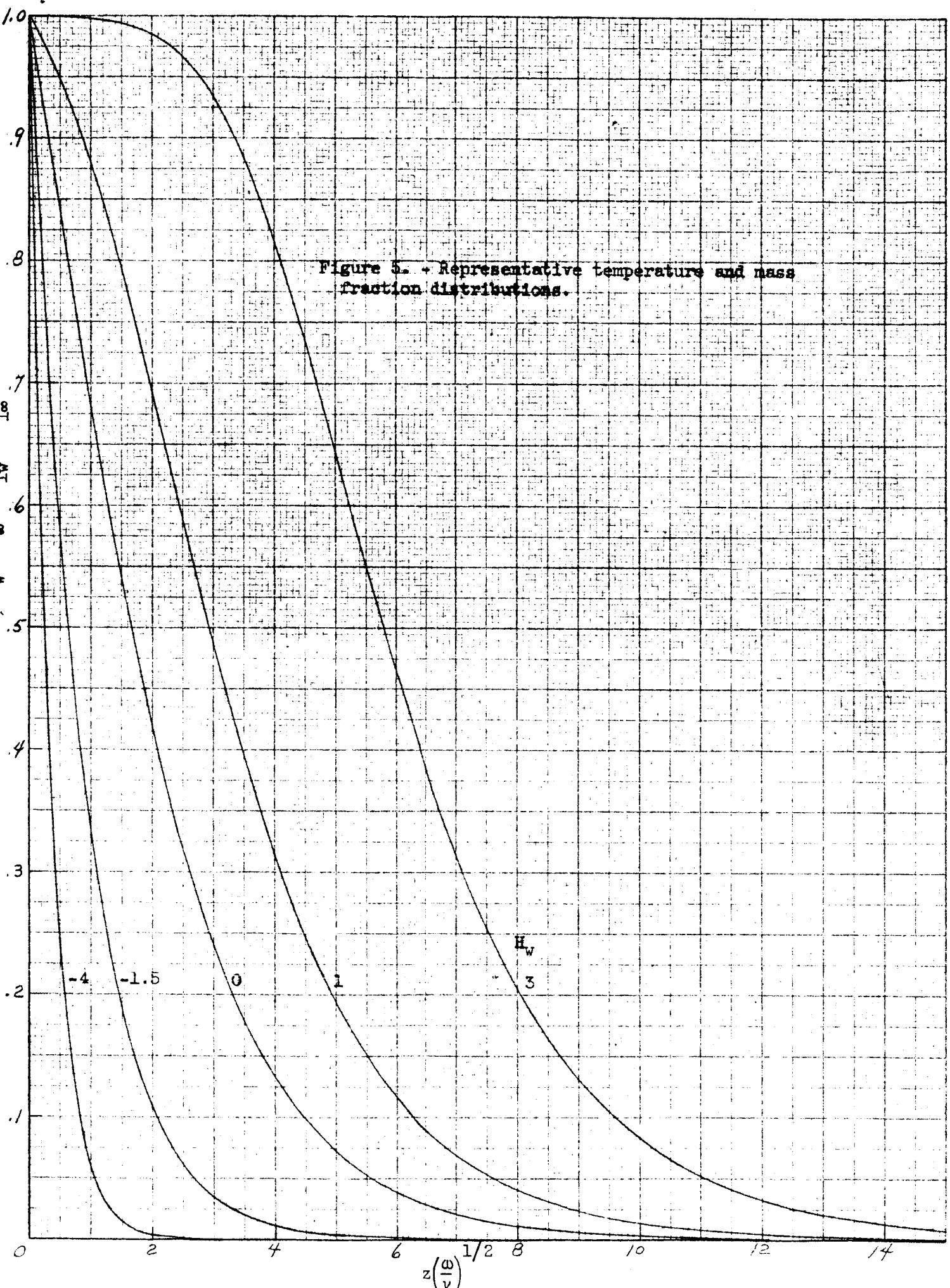
K+S 10 X 10 TO THE 1/2 INCH
MADE IN U.S.A.
KEUFFEL & ESSER CO.



$$\frac{T - T_{\infty}}{T_w - T_{\infty}} = \frac{W_1 - W_{1\infty}}{W_{1w} - W_{1\infty}}$$

K&E
10 X 10 TO THE 1/2 INCH
359-12
HEUPPEL & ESSER CO.
MADE IN U.S.A.

Figure 5. - Representative temperature and mass fraction distributions.



$$\frac{2\tau_r}{\rho r(\nu\omega^2)^{1/2}} = [-H''(0)]$$

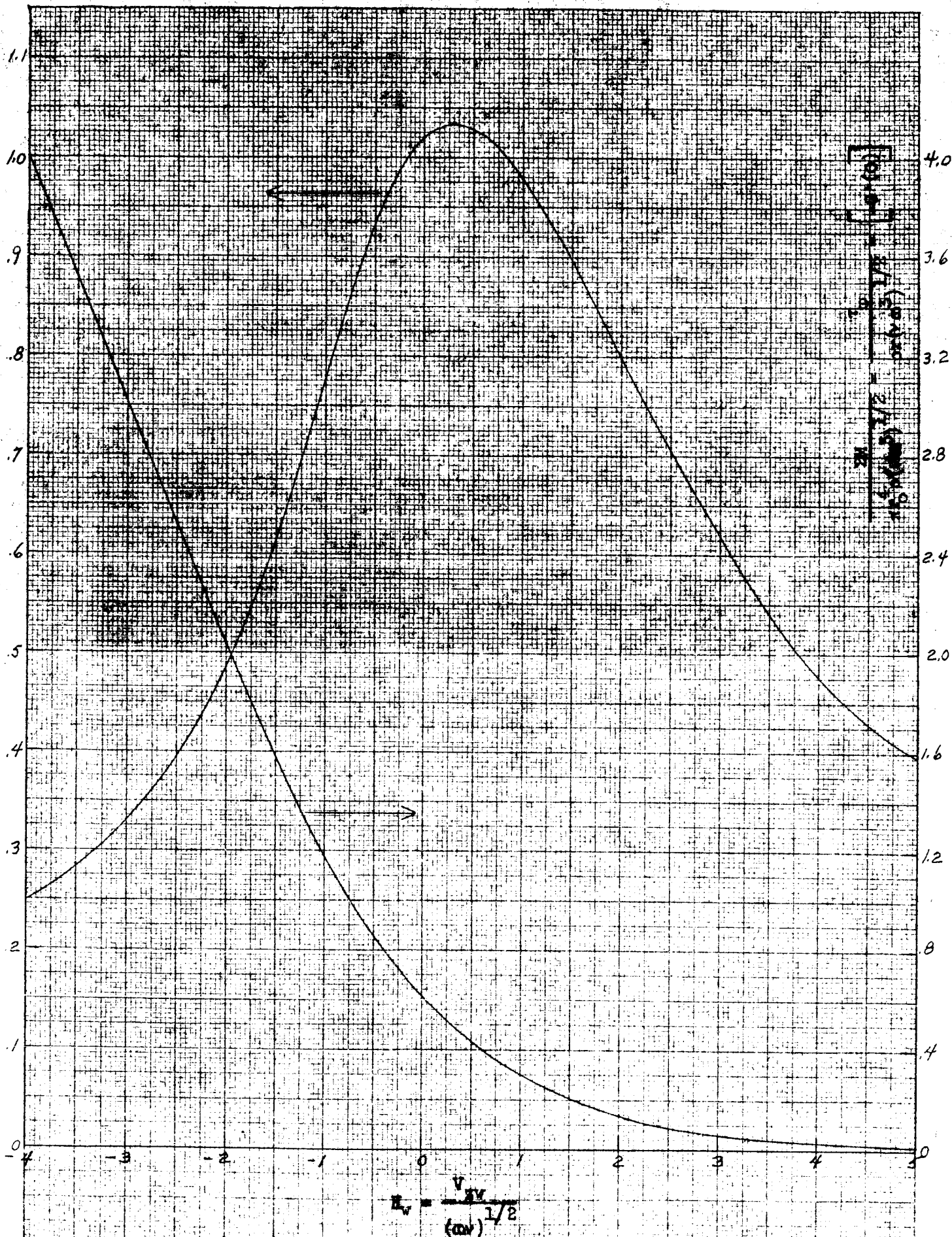


Figure 6. - Torque and shear stress results as a function of fluid injection (or withdrawal).

$$Nu = [-\theta'(0)] = [-\phi'(\phi)]$$

K&S
10 X 10 TO THE 1/2 INCH
KEUFFEL & ESSER CO.
359.12
MADE IN U.S.A.

28

24

20

16

12

8

4

$$H_w = \frac{V_{zw}}{(\omega\nu)^{1/2}}$$

-4

-3

-2

-1

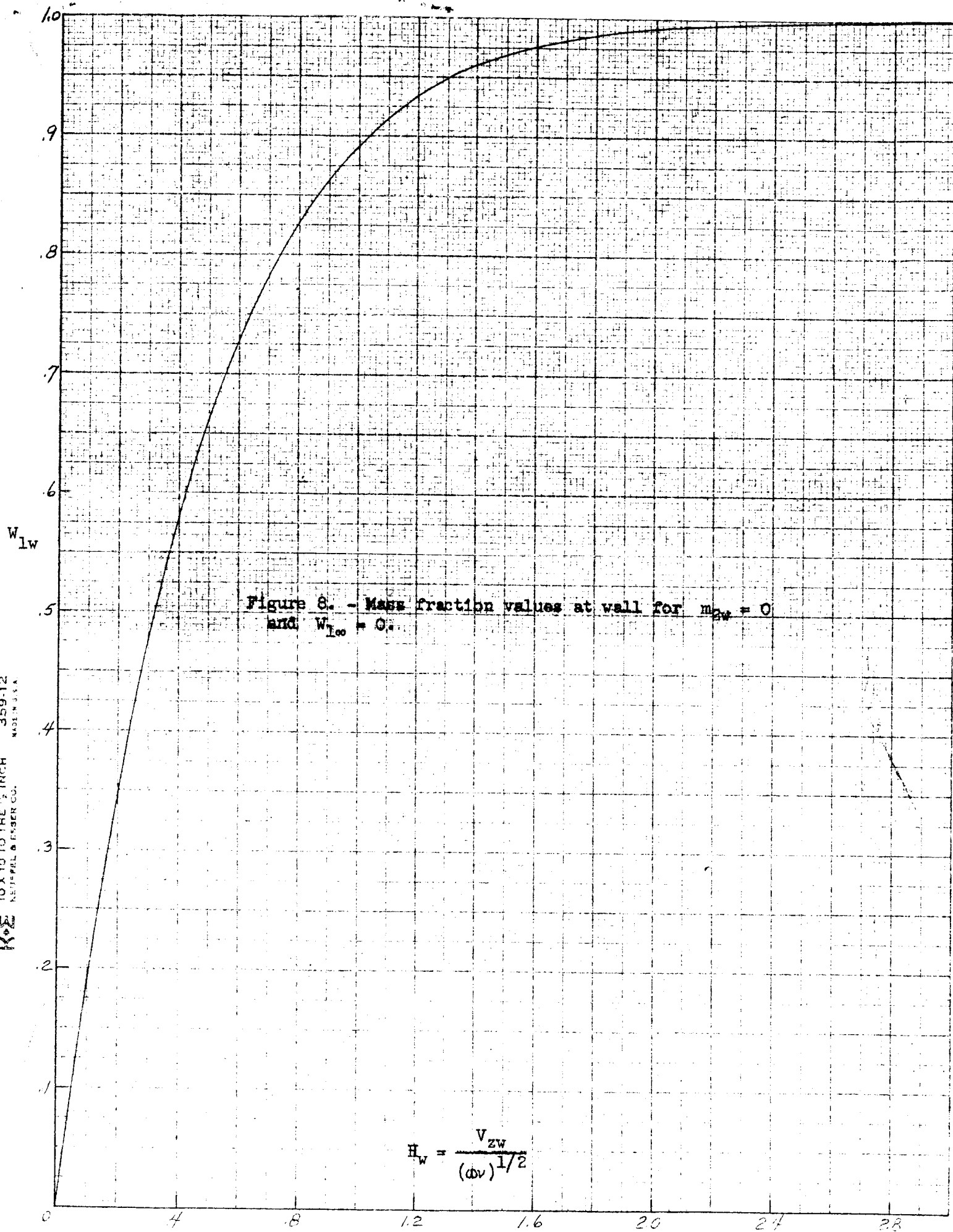
0

1

2

3

Figure 7. - Nusselt number results as a function of fluid injection (or withdrawal).



$$H_w = \frac{V_{zw}}{(\phi v)^{1/2}}$$